Available online at www.sciencedirect.com

ScienceDirect

Energy Procedia 67 (2015) 108 – 115

Energy Procedia

5th Workshop on Metallization for Crystalline Silicon Solar Cells

Optimized stencil print for low Ag paste consumption and high conversion efficiencies

H. Hannebauer[a,*], S. Schimanke[a], T. Falcon[b], P. P. Altermatt[c], T. Dullweber[a]

[a]*Institute for Solar Energy Research Hamelin (ISFH), Am Ohrberg 1, D-31860 Emmerthal, Germany*
[b]*ASM Assembly Systems Ltd, 11 Albany Road, Weymouth, DT4 9TH, U.K*
[b]*Department of Solar Energy, Institute of Solid-State Physics, Leibniz University Hannover, Appelstrasse 2, D-30167 Hannover, Germany*

Abstract

We evaluate industrial-type PERC solar cells applying a dual printed front grid with stencil printed Ag fingers. We vary the Ag paste consumption for the finger print between 8.4 mg and 120.4 mg per 156 × 156 mm² wafer (weighted after printing before drying) by using polyurethane squeegees with different shore hardness as well as a metal squeegee and by varying the printing pressure to obtain different finger heights. The busbar consumes additional 19.5 mg Ag paste. We obtain average finger heights from 5.9 µm up to 24.3 µm for 55 µm to 65 µm wide fingers. The resulting PERC solar cells show an average efficiency of 20.2% for finger paste consumptions above 60 mg. In contrast, a strong reduction of the conversion efficiency with less than 60 mg finger paste consumption is observed since the increased series resistance reduces the *FF*. By analytical modelling, we compare the calculated series resistance to the experimental data and observe a good accordance for more than 40 mg finger paste consumption whereas the experimental series resistance slightly exceed the modelled values below 40 mg. In addition, we use numerical simulations to investigate the series resistance dependence on the finger height which shows higher experimental values for finger height below 10 µm. The deviation of the measured series resistance and the two modelled cases is mostly due to inhomogeneous distribution of finger height profiles and finger interruptions on the solar cells with front finger paste consumption of less than 40 mg. For finger paste consumption below 60 mg, we find that also the specific contact resistance increases. A physical model of the root cause for this dependence still has to be found.

Peer-review under the responsibility of Gunnar Schubert, Guy Beaucarne and Jaap Hoornstra

Keywords: Silicon solar cell; Screen-printing; Metallization; Dual print; PERC; Paste consumption;

* Corresponding author. Tel.: +49-5151-999-637; fax: +49-5151-999-400.
E-mail address: hannebauer@isfh.de

Peer-review under the responsibility of Gunnar Schubert, Guy Beaucarne and Jaap Hoornstra
doi:10.1016/j.egypro.2015.03.294

1. Introduction

Industrial-type passivated emitter and rear cells (PERC) typically apply a screen-printed silver (Ag) front contact with a single print process using a mesh screen resulting in a paste consumption between 100 mg and 140 mg per 156 × 156 mm² wafer [1]. Due to the strongly improved rear side of PERC cells [2], future efficiency increases are expected to originate from optimization of the front side grid [3,4]. In addition to the efficiency improvement, reducing the Ag paste consumption is a further important contribution to minimize the module cost per watt peak. Dual print [5] of the Ag front grid is a promising technique to meet both objectives. The dual print process applies two printing steps. First, the busbars are printed with a non-firing through Ag paste using an optimized mesh screen for lower paste consumption. Then, the fingers are printed with a stencil [6] which features 100% open area in the aperture. This leads to a benefit of excellent paste transfer efficiency and line height uniformity when compared to a mesh screen´s typical 60% open area [7]. Thus, dual print provides a smooth finger profile in combination with a fine line printed silver finger width while maintaining a sufficient finger height in order to reduce resistive losses. Previous work on dual print demonstrated an efficiency up to 19.8% with an Ag paste consumption of 67.7 mg [8] as well as an efficiency of 21.2% with 74 mg Ag paste consumption applying a 5 busbar front grid [4].

In this paper, we investigate the dependence of the conversion efficiency on the finger paste consumption of PERC solar cells with a homogeneously diffused emitter and a dual printed front grid using a 40 µm stencil aperture. In order to achieve high efficiencies with a low Ag paste consumption, we use polyurethane squeegees with different shore (S) hardness as well as a metal squeegee and vary the printing pressure to obtain different finger heights. We measure the resulting Ag paste consumption after printing before drying, the resistance contribution of the front metallization, and all IV parameters of the final PERC solar cells. In addition, we analyze the experimental series resistance values by analytical calculations, while their dependence on the finger profile is modelled with numerical simulations.

2. Influence of stencil printing parameters on Ag paste consumption and front grid resistances

In the first printing step, a non-firing through Ag paste is printed with a standard rectangular shaped 3 busbar design resulting in an Ag paste consumption for the busbars of 19.5 mg after printing prior to drying. The subsequently applied nickel stencil has 101 fingers with an aperture of 40 µm. We use a commercially available silver paste for the finger print in this study. We test polyurethane squeegees with S hardness of 75A, 80A and 95A as well as a metal squeegee. The printing pressure is varied between 2.5 kg and 6 kg. The snap off and printing speed is kept constant. These printing variations lead to a measured Ag paste consumption on a cell after printing prior to drying for the finger print between 8.4 mg and 120.4 mg.

The finger profiles obtained with the different printing parameters are analyzed with a Wyko NT9100 optical profilometer. Images of the printed Ag fingers for three exemplary profiles are displayed in Fig. 1 a) – c). The min./max. values are derived from the mean values of the highest and lowest finger heights at three different positions of the solar cell. The printed finger width is 55 µm using polyurethane squeegees and 65 µm using the metal squeegee. We calculate the average finger height by measuring the finger profile over a finger length of

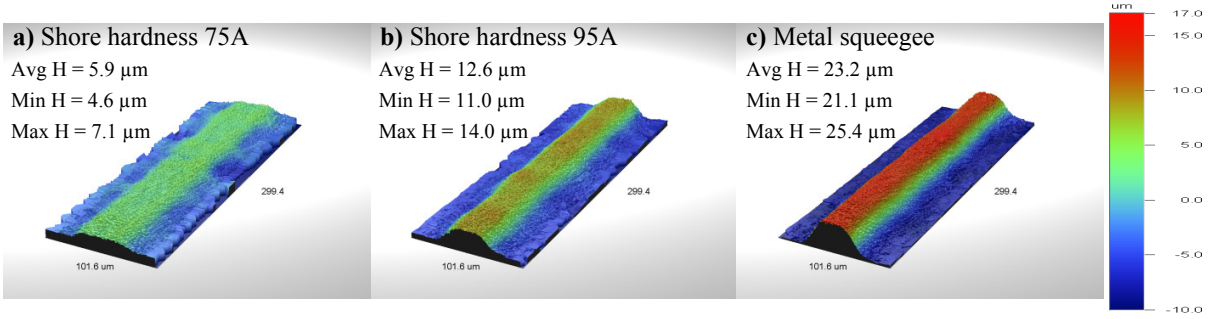

Fig. 1: Finger profiles measured with an optical profilometer printed using a) shore hardness 75A squeegee, b) shore hardness 95A squeegee and c) metal squeegee. “H” denotes the measured finger height.

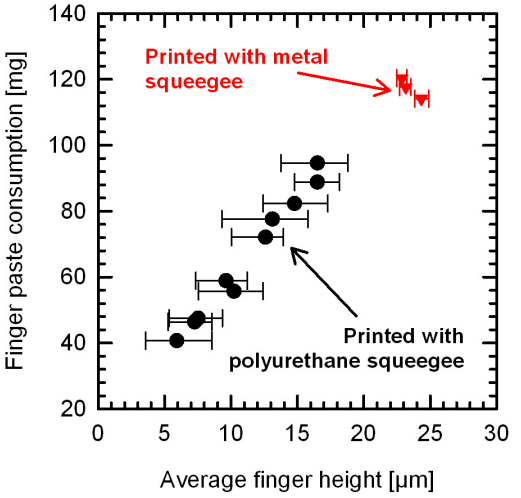

Fig. 2: Finger paste consumption versus average finger height measured with an optical profilometer. The data points present the average finger height of finger profiles on three different positions on a cell. The error bars are chosen according to the min./max. values of average finger heights at the three positions.

0.5 mm at the bottom, the mid, and the top of the cell between the busbars in parallel to the squeegee of the finger stencil print. The measured average finger heights are displayed in Fig. 2 and show a nearly linear decrease of the finger paste consumption with decreasing finger height. We achieve the greatest average finger height of 24.3 µm with a finger paste consumption of 114.1 mg using the metal squeegee. The metal squeegee in contrast to the soft polyurethane squeegee does not penetrate into the stencil opening during the print and hence achieves the greatest finger heights. The smallest measured average finger height is 5.9 µm with a finger paste consumption of 40.7 mg using S hardness 75A squeegee. Finger heights with finger paste consumption below 40 mg are not measured because these cells have many finger interruptions and a very inhomogeneous printing image which would lead to an incorrect measurement of the average finger height. The error bars are chosen according to the min./max. values of average finger heights at the three measurement positions which indicates the finger height uniformity across the

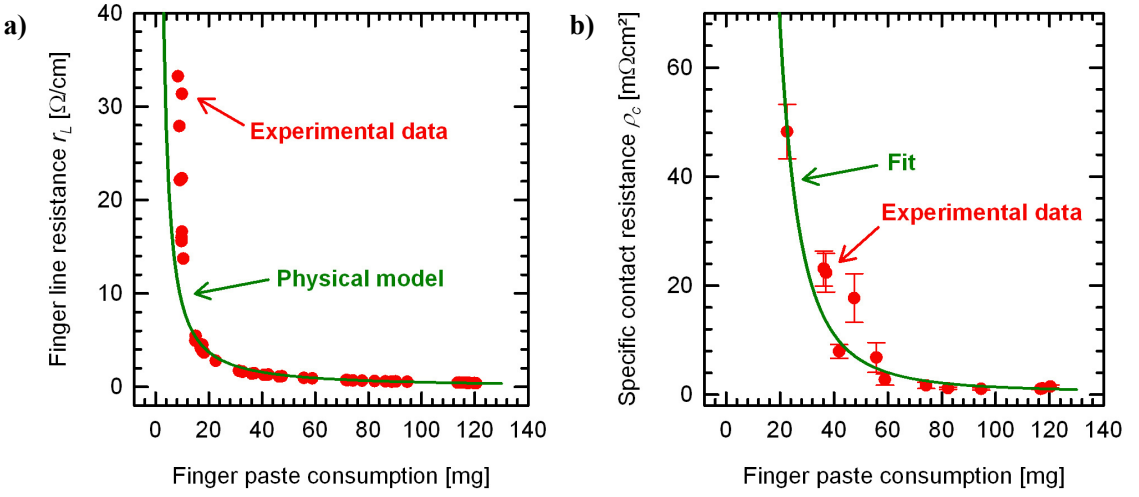

Fig. 3: Measured a) finger line resistance r_L and b) specific contact resistance ρ_c versus finger paste consumption. The green lines refer to fitted curve of the experimental data with a) a physical model and b) a mathematical power function. The error bars in b) show the standard deviation of the measured ρ_c on the cells.

cell. The cells printed with the metal squeegee show a very uniform distribution with a min./max. variation between 0.35 µm and 0.55 µm. However, the min./max. variation for the cells using the polyurethane squeegees is in the range of 1.3 µm and 3.8 µm. The non-uniform finger heights across the wafer could be caused by an imperfectly flat mounted polyurethane squeegee or by suboptimal chosen printing parameters which we have to investigate in more detail. All printing options show a nearly flat surface profile along the finger length for single measurements with a standard deviation between 0.31 µm and 1.56 µm.

In addition, we measure the finger line resistance r_L as well as the specific front contact resistance ρ_c to the emitter. For the finger line resistance shown in Fig 3a), we measure the resistance between the busbars taking into account the distance between the busbars as well as the number of fingers. We fit the experimental data by assuming that the finger line resistance depends on the specific resistivity of the Ag paste divided by the finger cross-section area. For the calculation of the cross-section area we use a trapezoidal shaped finger with a bottom finger width of 62 µm and a top surface width of 21.7 µm to match the finger profile measurements in Fig. 1. To fit the model with the experimental data, the specific resistivity is set to 4 µOhmcm which is comparable to the data sheet which reports 3 µOhmcm for that Ag paste. The lowest r_L of 0.39 Ω/cm is obtained with the highest finger paste consumption of 120.4 mg. The specific contact resistance in Fig. 3b) is measured using the transfer length method TLM [9]. The measurement is done on 10 mm narrow strips to ensure that the varying finger line resistance does not influence the TLM results. The measured contact resistance values are corrected by outliers which may results from finger interruptions at low Ag paste consumption. The PERC solar cells show an average ρ_c of 1.27 mΩcm² for a finger paste consumption above 60 mg. However, the specific contact resistance increases strongly for a finger paste consumption below 60 mg. We fit the experimental data by a mathematical power function. The fitted curves in these graphs are used later for the calculation of the total series resistance of PERC solar cells. As the dependence of the specific contact resistance on the paste consumption and finger height is unexpected, we will investigate the root cause for the dependence in the future in more detail.

3. PERC solar cells with dual print

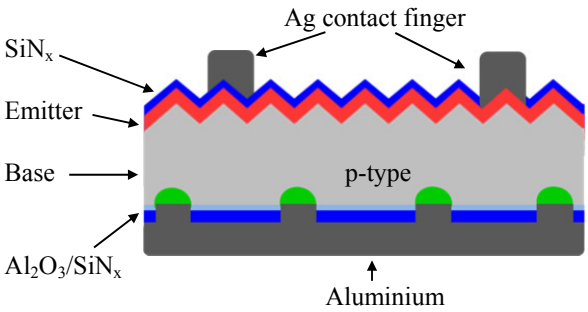

Fig. 4: Schematic drawing of the PERC silicon solar cell with printed Ag front and Al rear contacts.

We use 2 Ωcm, 156 × 156 mm², boron-doped Czochralski-grown silicon wafers with a thickness of 180 µm. The process flow is described in detail in [2]. Here we just highlight the most important process steps. After cleaning and damage etching, we deposit a protection layer on the rear side before texturing in an alkaline batch process. After a homogenously diffused phosphorus emitter of 65 Ω/sq sheet resistivity, the protection layer is removed by wet chemistry, followed by a cleaning step. The rear side is passivated by an atomic-layer deposited (ALD) Al_2O_3/SiN_x layer stack, whereas the front side is covered with a PECVD SiN_x antireflective layer. Line-shaped laser contact openings (LCO) are formed on the rear side using a picosecond laser with a wavelength of 532 nm. We use a DEK Eclipse printer for the dual print of the silver front side metallization and evaluate different printing parameters as described above. After the front grid print, the rear side of the PERC cell is screen-printed full-area with aluminium (Al) paste. A drying process in a belt furnace completes each printing step. The front and the rear contacts are fired in a conventional belt furnace during which the Al paste locally alloys with the silicon wafer at areas where the rear

passivation has been removed by laser ablation. A schematic drawing of the resulting PERC solar cell is shown in Fig. 4.

Figure 5 a) – d) shows the conversion efficiency η as well as the open-circuit voltage V_{oc}, the short-circuit current-density J_{sc}, and the fill factor FF of the resulting PERC solar cells versus the finger paste consumption. For finger paste consumptions above 60 mg, the PERC solar cells show an average efficiency of 20.2%. However, with less than 60 mg finger paste consumption a strong reduction of the conversion efficiency is observed since the increased series resistance reduces the FF. Most of these solar cells obtained an average value of 655 mV for the V_{oc} and 38.4 mA/cm² for the J_{sc}. For finger paste consumptions below 20 mg, the PERC cells show a reduced V_{oc} and J_{sc} caused by many finger interruptions.

The grey star-shaped data point in Fig. 5 a) – d) refers to an optimized diffusion process and shows the highest conversion efficiency with dual print. For this cell, we use another $POCl_3$ diffusion which leads to a final sheet resistance of 100 Ω/sq. Additionally, standard rectangular shaped 3 busbar design is changed to a segmented 3 busbar design [8] which leads to a reduced fraction of the Ag paste consumption of the busbars to the total front side

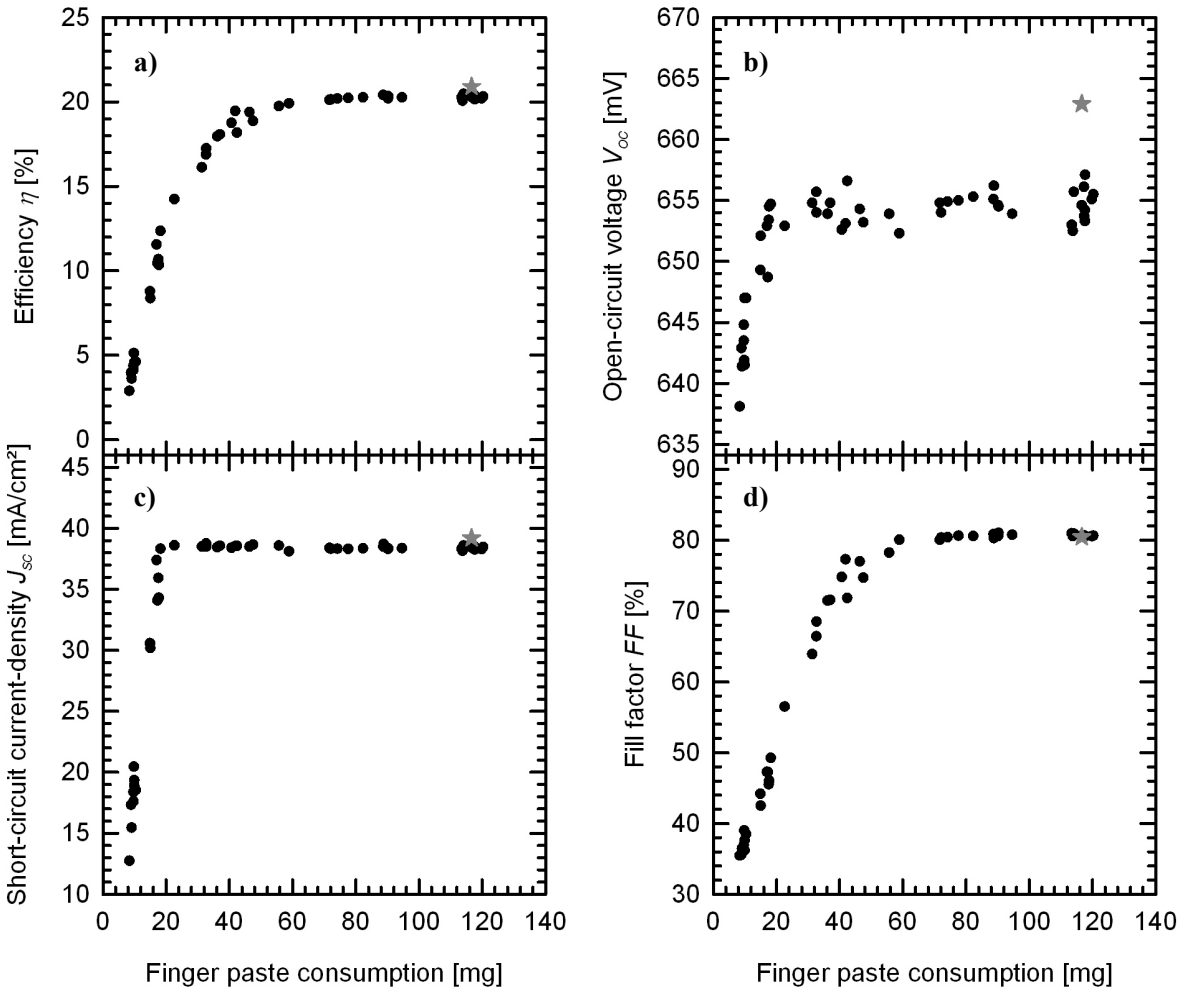

Fig. 5: Conversion efficiency η (a), open circuit voltage V_{oc} (b), short circuit current J_{sc} (c) and fill factor FF (d) of PERC solar cells versus the finger paste consumption. The conversion efficiency of PERC cells starts to strongly decrease for finger paste consumptions below 40 mg. The grey star-shaped data point refers to the highest efficiency of 20.9% using a slightly increased emitter sheet resistance compared to the other PERC solar cells.

Ag paste consumption. In this case we use a commercially available stencil Ag paste. This PERC solar cell achieves a conversion efficiency of 20.9% with V_{oc} of 663 mV, J_{sc} of 39.2 mA/cm² and a fill factor FF of 80.4% and requires 136.2 mg Ag paste consumption which can divided into 122.0 mg for the finger and 14.2 mg for the busbar print.

4. Modelling of the series resistance

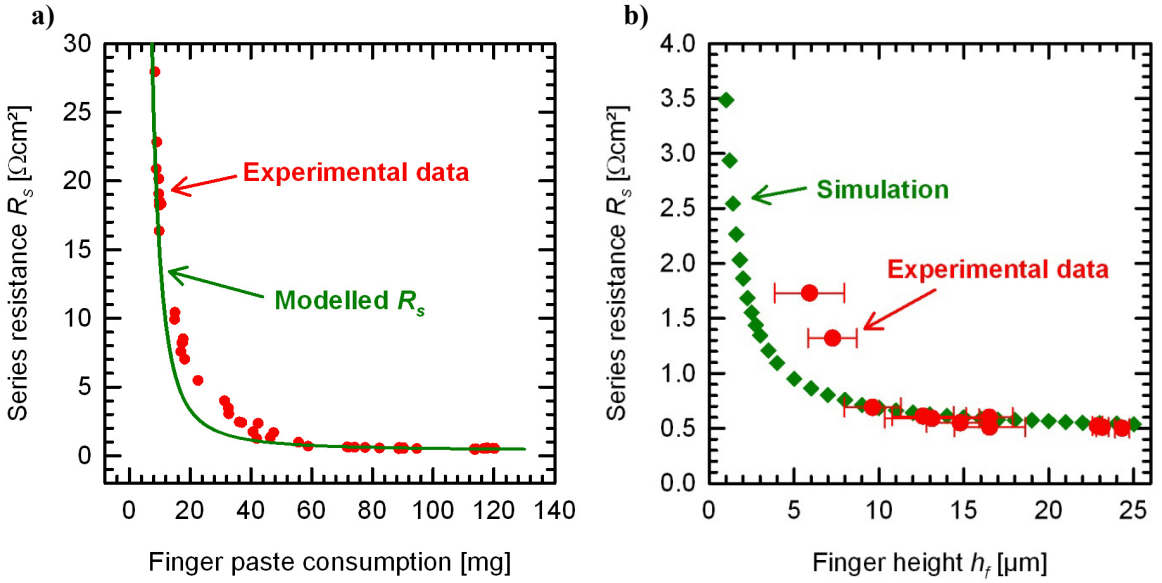

Fig. 6: Comparison of the experimental data for the series resistance versus a) the finger paste consumption to a calculated R_s from analytical model b) the finger height to R_s from numerical and network simulations.

In order to analyze the dependence of the series resistance R_s on the finger paste consumption, we compare the analytically calculated series resistance to the experimental data. We use the following equations to model the series resistance [10]:

$$R_s = R_{finger} + R_{contact} + R_{emitter} + R_{base} + R_{rear} \tag{1}$$

The finger resistance is described by

$$R_{finger} = \tfrac{2}{3} r_L \cdot l_f \cdot A_{uc} \tag{2}$$

with the finger line resistance r_L and the finger length l_f which corresponds to the half distance between two neighbouring busbars. The area of the unit cell A_{uc} is defined as the half of the finger pitch s times a which corresponds to the half pitch between two neighbouring busbars. The front contact resistance is given by

$$R_{contact} = \frac{\sqrt{R_{sheet} \cdot \rho_c}}{l_f} \coth\left(\frac{w_f}{2} \sqrt{\frac{R_{sheet}}{\rho_c}} \right) \cdot A_{uc} \tag{3}$$

with the specific contact resistance ρ_c of the Ag paste to the emitter, the emitter sheet resistance R_{sheet} and the finger width w_f. We assume constant values of $R_{emitter}$, R_{base}, and R_{rear} and use the fitted curves for finger line resistance r_L and specific contact resistance ρ_c values shown in Fig. 3a) and b) to calculate the series resistance versus the finger paste consumption. Figure 6a) shows the series resistance of the PERC solar cells which strongly increases for front side finger paste consumptions below 40 mg. The green line refers to modelled R_s values applying equations 1) to

3). We observe a good accordance for more than 40 mg finger paste consumption whereas the experimental series resistance values slightly exceed the modelled values below 40 mg. The root cause for this slight discrepancy still has to be analyzed.

In addition, we compare the measured series resistance to series resistance values obtained by numerical simulations. Firstly, we simulated the IV curve of a small irreducible domain of a PERC cell using the software Sentaurus Device [11,12]. Secondly, we simulated the IV curve of the entire cell by a SPICE simulation [13,14], where we lay out the irreducible domain multiple times like tiles and connect them with resistances that represent segments of the front metal fingers and the busbars. In the SPICE simulation, we use a specific Ag paste resistivity of 3 μΩcm, 101 fingers and three busbars. To compute the total series resistance of the metallization, the cross section area of the metal fingers is modelled assuming a trapezoidal shaped finger with a bottom finger width of 62 μm and a top surface width of 21.7 μm. The finger height is assumed to be perfectly uniform across the finger length which is a valid approximation for stencil-printed fingers. To simulate the series resistance dependence on the finger height, we vary the finger height from 1 μm to 25 μm. In Fig. 6b), a comparison of the measured and simulated series resistance versus the finger height is displayed. The error bars are chosen according to Fig. 2. The simulation indicates a further possible reduction of the Ag paste consumption for high cell efficiencies shown by the simulated series resistance below 1 Ωcm² for a uniform finger height of 5 μm across the cell which corresponds to 40 mg finger paste consumption. The series resistance dependence on the finger height obtained with numerical simulations shows higher experimental values for finger heights below 10 μm. The rather strong deviation has two main reasons. First, we determined an increased specific contact resistance with reduced finger paste consumption shown in Fig. 3b) whereas ρ_c is kept constant at 1.5 mΩcm² for all finger heights in the simulation shown in Fig. 6b). The second possibility is that the observed inhomogeneous finger height on different cell positions as well as finger interruptions for low finger paste consumption produces local higher series resistances that are not included in the grid simulation.

5. Conclusion

This paper systematically evaluates the influence of the Ag paste consumption for the finger print on the conversion efficiency by varying the finger height of dual printed PERC solar cells. With different printing parameters we vary the front finger paste consumptions after printing prior to drying between 8.4 mg and 120.4 mg where the busbars consume additional 19.5 mg. The average finger height varies between 5.9 μm and 24.3 μm accordingly. For finger paste consumptions above 60 mg, the PERC solar cells show an average efficiency of 20.2%. However, with less than 60 mg finger paste consumption a strong reduction of the conversion efficiency is observed since the increased series resistance reduces the *FF*. By analytical modelling, we compare the calculated series resistance to the experimental data. For more than 40 mg Ag paste consumption we observe a good accordance between the series resistance values. However, for paste consumptions below 40 mg the experimental series resistance values slightly exceed the modelled values. The series resistance dependence on finger height obtained with numerical simulations shows higher experimental values for finger heights below 10 μm. The deviation of the measured series resistance and the two modelled cases for low paste consumption and small finger heights, respectively, is most likely due to inhomogeneous distribution of finger height profiles and finger interruptions on the solar cells with front finger paste consumption of less than 40 μm. In addition, we find that the specific contact resistance strongly increases for finger paste consumptions below 60 mg. A physical model of the root cause for this dependence still has to be found.

Acknowledgements

This work was funded by the German Federal Ministry for the Environment, Nature Conservation, Building and Nuclear Safety within the R&D project HighScreen in cooperation with SolarWorld Innovations GmbH, RENA GmbH, SINGULUS TECHNOLOGIES AG and Heraeus Precious Metals and by our industry partner ASM Assembly Systems.

References

[1] ITRPV Working Group. International Technology Roadmap for Photovoltaic, 2013 Results. Revision 1, March 2014

[2] Dullweber T, Gatz S, Hannebauer H, Hesse R, Schmidt J, Brendel R. Towards 20% efficient large-area screen-printed rear-passivated silicon solar cells. *Prog. Photovolt.: Res. Appl.* **20**: 2012, p. 630-638.

[3] Metz A, Adler D, Bagus S, Blanke H, Bothar M, Brouwer E, Dauwe S, Dressler K, Droessler R, Droste T, Fiedler M, Gassenbauer Y, Grahl T, Hermert N, Kuzminski W, Lachowicz A, Lauinger T, Lenck N, Manole M, Martini M, Messmer R, Meyer C, Moschner J, Ramspeck K, Roth P, Schönfelder R, Schum B, Sticksel J, Vaas K, Volk M, Wangemann K. Industrial high performance crystalline silicon solar cells and modules based on rear surface passivation technology. *Sol. Energy Mater. Sol. Cells* **120**: 2014, p. 417-425.

[4] Hannebauer H, Dullweber T, Baumann U, Falcon T, Brendel R. 21.2%-efficient fineline-printed PERC solar cell with 5 busbar front grid. *Phys. Status Solidi RRL* **8** (8): 2014, pp. 675-679.

[5] Hoornstra J, Heurtault B. Stencil print applications and progress for crystalline silicon solar cells. *Proc 24th European Photovoltaic Solar Energy Conference*, Hamburg, Germany, 2009, p. 989-992.

[6] de Moor H.H.C, Weeber A.W, Hoornstra J, Sinke W.C. Fine-line screen printing for silicon solar cells. *6th Colorado Workshop*, Snowmass, 1996, p. 154-170.

[7] Falcon T. Ultra Fine Line Printing for Silicon Solar Cells….Mesh Screens or Metal Stencils? *Presentation at the 3rd Metallization Workshop*, Charleroi, Belgium, 2011.

[8] Hannebauer H, Dullweber T, Falcon T, Chen X, Brendel R. Record low Ag paste consumption of 67.7 mg with dual print. *Proc 4th Metallization Workshop, Energy Procedia* **43**: 2013, p. 66-71.

[9] Berger H.H. Models for contacts to planar devices. *Solid-State Electronics* **15**: 1972, p. 145-158

[10] Mette A. New concepts for front side metallization of industrial silicon solar cells. *PhD thesis,* Freiburg, Germany, 2007.

[11] Sentaurus User Manual, Synopsys Inc., Mountain View, CA, 2013.

[12] Altermatt P.P. Models for numerical device simulations of crystalline silicon solar cells - a review. *Journal of Computational Electronics* **10**: 2011, p. 314-330.

[13] Nagel L.W, Pederson D.O. Simulation program with integrated circuit emphasis (SPICE). *16th Midwest Symp. Circuit Theory*, Waterloo, ON, Canada, 1973.

[14] LTspice IV. (2011). [Online]. Available: http://www.linear.com/ designtools/software/ltspice.jsp: Linear Technology.